Results from Benchmark Testing at Pipeline Simulation Facility
September 13-16, 2004

APPLICATION OF REMOTE-FIELD EDDY CURRENT (RFEC) TESTING TO INSPECTION OF UNPIGGABLE PIPELINES

OTHER TRANSACTION AGREEMENT DTRS56-02-T-0001
SwRI® PROJECT 14.06162
OFFICE OF PIPELINE SAFETY
U.S. DEPARTMENT OF TRANSPORTATION

SOUTHWEST RESEARCH INSTITUTE®

October 2004

INTRODUCTION AND BACKGROUND

Many pipelines contain internal restrictions that do not allow the passage of conventional technology inspection pigs. The purpose of this project was to investigate the feasibility of a remote-field eddy current (RFEC) inspection method that utilizes either a unique collapsible excitation coil or a small rigid excitation coil that can pass through internal pipeline restrictions.

Remote-field eddy current testing is based on placing an excitation coil driven with alternating current in the pipe and thereby inducing eddy currents in the pipe wall. Sensors are placed adjacent to the pipe wall at a distance several coil diameters away from the exciter. At this "remote-field" location, the magnetic field from the excitation coil is very small, and the direct coupling from the coil into the sensors is minimal. At the sensor location, however, magnetic field components from the eddy currents have penetrated through the pipe wall to the OD and then back through the pipe wall to the ID. This field is detected by the sensors and is sensitive to material-loss defects because it has penetrated through the pipe wall.

Typically, it is desirable for the excitation coil to be only slightly smaller than the pipe ID, as this maximizes electromagnetic coupling into the pipe wall and maximizes sensitivity to defects. Sensors are typically positioned near the pipe wall and are configured as an array on collapsible arms. Two approaches initially considered in this project to allow an RFEC system to negotiate internal restrictions were to use (1) a full-size exciter coil that could fold to pass restrictions and then expand back to full size and (2) a rigid exciter coil of small diameter that could directly pass through restrictions. Because electromagnetic modeling and experimental results showed severe reductions in sensitivity with a small exciter coil, the approach chosen for this project was to develop and demonstrate an RFEC system with a full-size collapsible exciter coil.

This report describes benchmark testing of a laboratory breadboard RFEC system with a collapsible coil. The testing was performed during the period of September 13–16, 2004, at the Pipeline Simulation Facility in Columbus, Ohio.

EXPERIMENTAL SETUP

A laboratory breadboard RFEC system was configured for testing in 12-inch-diameter pipe. This system is shown in Figure 1. The system consists of a six-segment collapsible excitation coil and a single sensor coil that is mounted on a collapsible arm and spring-loaded against the pipe ID. The system uses two tripod-centering devices that are also spring-loaded against the pipe ID. The centering devices ride on elastomeric wheels, and one wheel drives an encoder that provides position information as the system travels down the pipe.
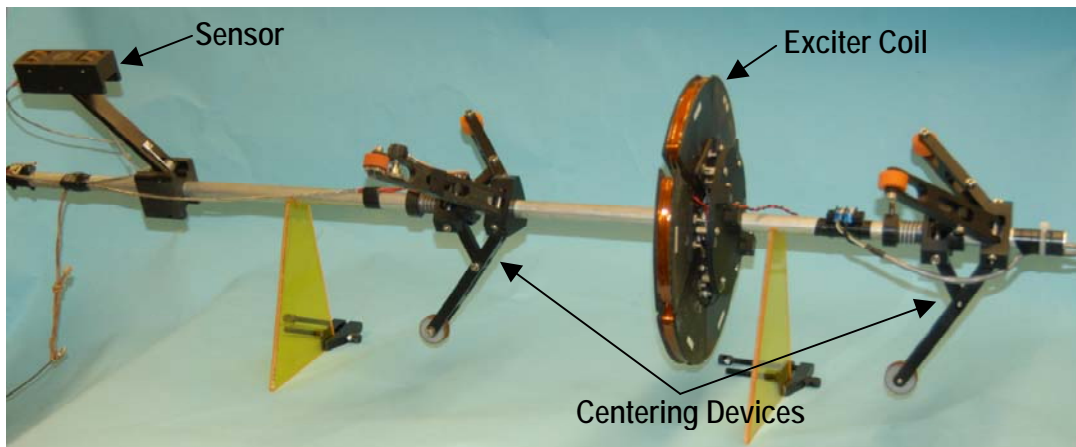

Figure 1. Laboratory breadboard RFEC system

Scanning of the pipe was performed using a winch to pull the RFEC system continuously through the pipe at a velocity of approximately 2 inches/second. Because the laboratory breadboard only uses one sensor instead of an array of sensors (which could be added in the future), it was necessary to change the angular position of the sensor and to repeat scans of the pipe so that all desired circumferential positions could be covered. In order to assure that angular position of the system was constant throughout each scan, a tensioned cable was positioned against the pipe ID, and a groove in one set of tripod wheels followed the cable.

Two 12-inch-diameter pipes, both having a nominal wall thickness of 0.375 inch, were tested: (1) a new 32-foot-long grade B seam-welded pipe containing machined defects and (2) a 48-foot-long seamless pipe containing three machined defects and natural corrosion that was removed from service (used). The new pipe contained two circumferential welds, and the used pipe contained one circumferential weld. Calibration defects machined into the pipes are as follows:

32-foot new pipe:	1.2-inch long, 3.0-inch wide, 0.3-inch deep (80% wall loss)
48-foot used pipe:	1.0-inch diameter, 0.305-inch deep
	1.5-inch diameter, 0.193-inch deep
	1.5-inch diameter, 0.175-inch deep

The calibration defects were visible, but other regions of the pipes were masked so that the tests on those regions were blind to the inspectors. The new pipe had flaws machined along two lines,

180 degrees apart. In this pipe, multiple scans of the system were made with the sensor coil positioned in 0.5-inch circumferential increments ±3 inches on each side of each line. For the used pipe, scans were made in 0.5-inch increments ±4.5 inches on each side of a single line. All scans were initiated at end A of each pipe.

The DOE requested analysis of the data in specified regions along the length of each pipe. The data requested in each region include start, end, total length, width, and maximum depth of metal loss. The intent of the original SwRI project was to show feasibility of flaw detection with the RFEC system; therefore, procedures for flaw characterization (primarily depth determination) were not included. Nevertheless, to support this benchmarking demonstration, cursory flaw characterization procedures were developed.

The basis of the data analysis procedure was a determination of relationships (1) between signal amplitude and cross-sectional area of the defect (assuming that the cross-sectional shape was defined by the arc of a circle) and (2) between signal spatial extent and spatial extent of the flaw. These relationships were determined from calibration defects in pipes tested during the benchmark testing, as well as a test pipe at SwRI. (It should be noted that signals from the new pipe were larger than those from the used or the SwRI pipe, probably because it is lower strength and has higher permeability. Therefore, the calibration for this pipe was adjusted accordingly.) Based on signal amplitude, the cross-sectional area of the defect was determined. Then, based on signal spatial extent, the width of the flaw was determined. The flaw depth was then calculated by fitting the arc of a circle to these parameters and calculating the resulting depth. It should be noted that more sophisticated analysis routines could likely produce more accurate results.

TEST RESULTS

Signals from scans of the new pipe along lines 1 and 2 are shown in Figures 2 and 3, respectively. A waterfall plot of all scans is shown at the top of the figure, and a 2-D color image of the same data is shown at the bottom. The horizontal axis is distance in inches from end A of the pipe, and the vertical axis represents circumferential position in inches with respect to the centerline of the designated scan area. The data were analyzed in the regions along the length of the pipe, as requested according to the "Search Region" column indicated in the reporting table supplied by DOE. Data outside these regions are designated in the figures, but were not analyzed; these include signals from the circumferential grooves near each end of the scans, signals from the two welds, and signals from the calibration defect (inside red rectangle). Signals from defects are indicated by red ellipses drawn in the waterfall plot; these signals are designated according to the search region in the table (e.g. MC02). Four strong signals were observed, and the calculated characteristics of these flaws are shown in the table. The calculated characteristics of the calibration flaw are also shown in the table. Two additional sets of signals were also observed, and these are designated as "Circumferential Indications" at the top of the figure. It is not clear if these are actual flaws because they persist around the entire circumference of the scanned area along both lines 1 and 2 in this pipe. These are either a circumferential defect or perhaps a local variation in pipe permeability or thickness.

Figure 3 shows four strong flaw signals along line 2 in the new pipe. In addition, the two circumferential indications observed in Figure 2 are observed, along with a third circumferential indication. Calculated flaw parameters are given in the table.

Figure 4 shows the data from the used pipe, and several differences are observed compared to the data from the new pipe. There is considerable variation in the signal background level, as can be seen from the overall changes in color in the color image (e.g. large patches of blue, yellow, and red) and shifts in the baselines of the individual scans in the waterfall plot. There are also circumferential "stripes" in the signal, as seen in the color image. These variations are likely caused by the manufacturing process of the seamless pipe that results in variations in thickness and possibly permeability of the pipe. In order to remove the overall changes in background level, the data were subjected to a high-pass filtering operation, and the result is shown in Figure 5. Although the "stripes" are still evident in the color image, the flaw signals are more apparent.

As with the new pipe, the calibration flaws are designated by red rectangles in the waterfall plot, and signals from unknown flaws are designated by red ellipses. In some cases, it was difficult to discriminate flaw signals from the circumferential background signals that resulted in the "stripes." Generally, signals that were sharply varying and occurred on several, but not all, circumferential scans were considered to be from flaws, and signals that were more slowly varying and occurred at the same circumferential location for all of the scans were not considered as flaws. A more sophisticated analysis may yield better results.

Several flaw areas are designated in Figures 4 and 5, and the calculated flaw characteristics are shown in the table. Note that in region T11, two different flaws were detected, and these are designated by two ellipses designated T11a and T11b. It is possible that the T11b region is actually part of the same defect designated T12, but these were designated separately to fit within the defect regions requested in the table. Two additional defect areas designated A and B were also found; these are shown in Figures 4 and 5 but were not included in the table because they were outside the regions where flaw reporting was requested. Defect T13 is unusual in that it only appears at a single circumferential position; however, it was designated as a defect because of its large amplitude.

CONCLUSIONS

The collapsible RFEC system performed well with few problems during the benchmark testing. Signals were obtained from known calibration flaws in both new and used pipe, and numerous signals were obtained from flaws in blind areas of the pipe. A simplified flaw characterization procedure was developed, and flaw characteristics including length, width, and maximum depth were calculated based on signal characteristics. These characteristics were reported according to designated regions in the reporting table provided by DOE.
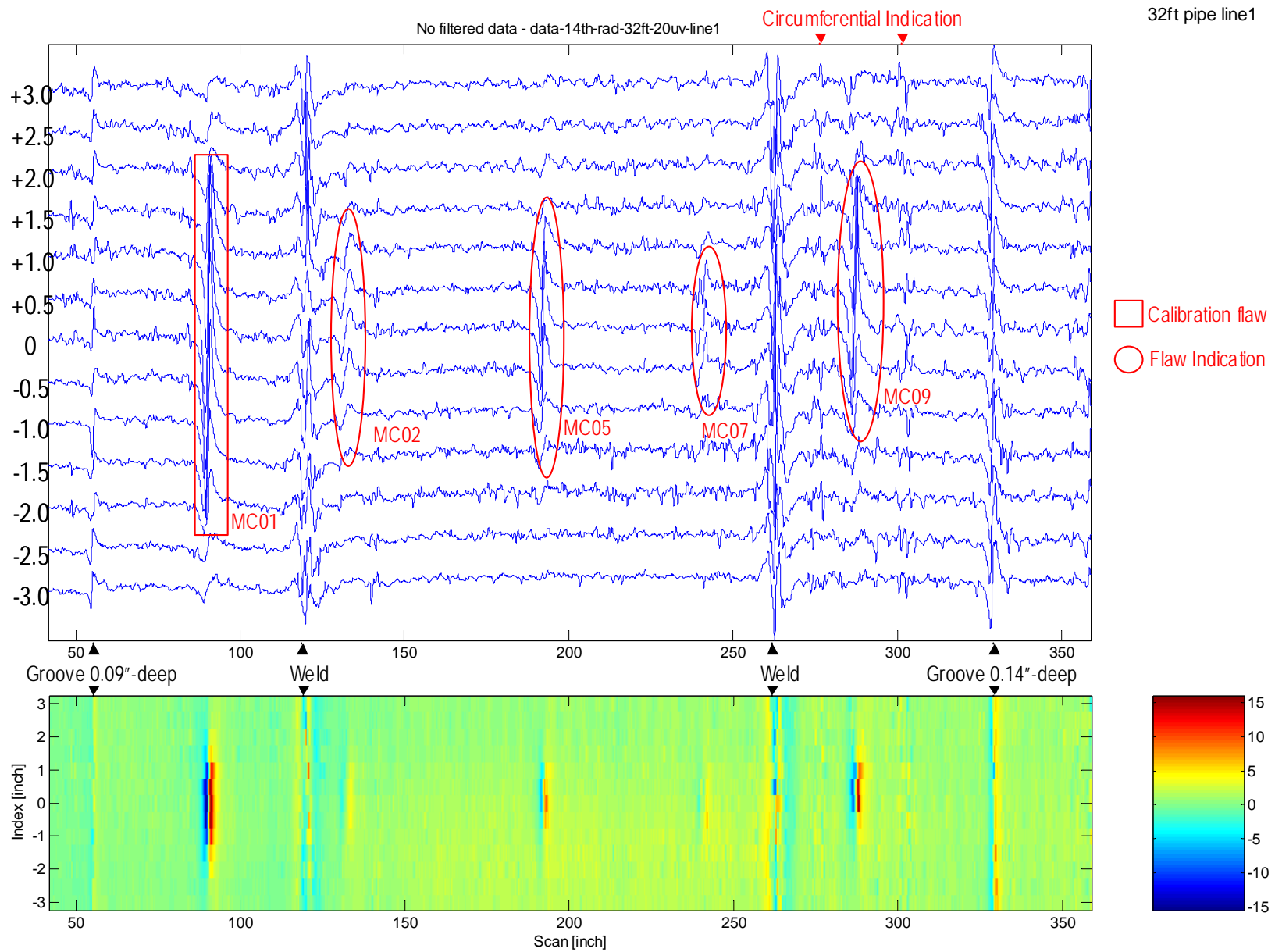
Figure 2. RFEC data from new seam-welded pipe with manufactured flaws — scan along Line 1
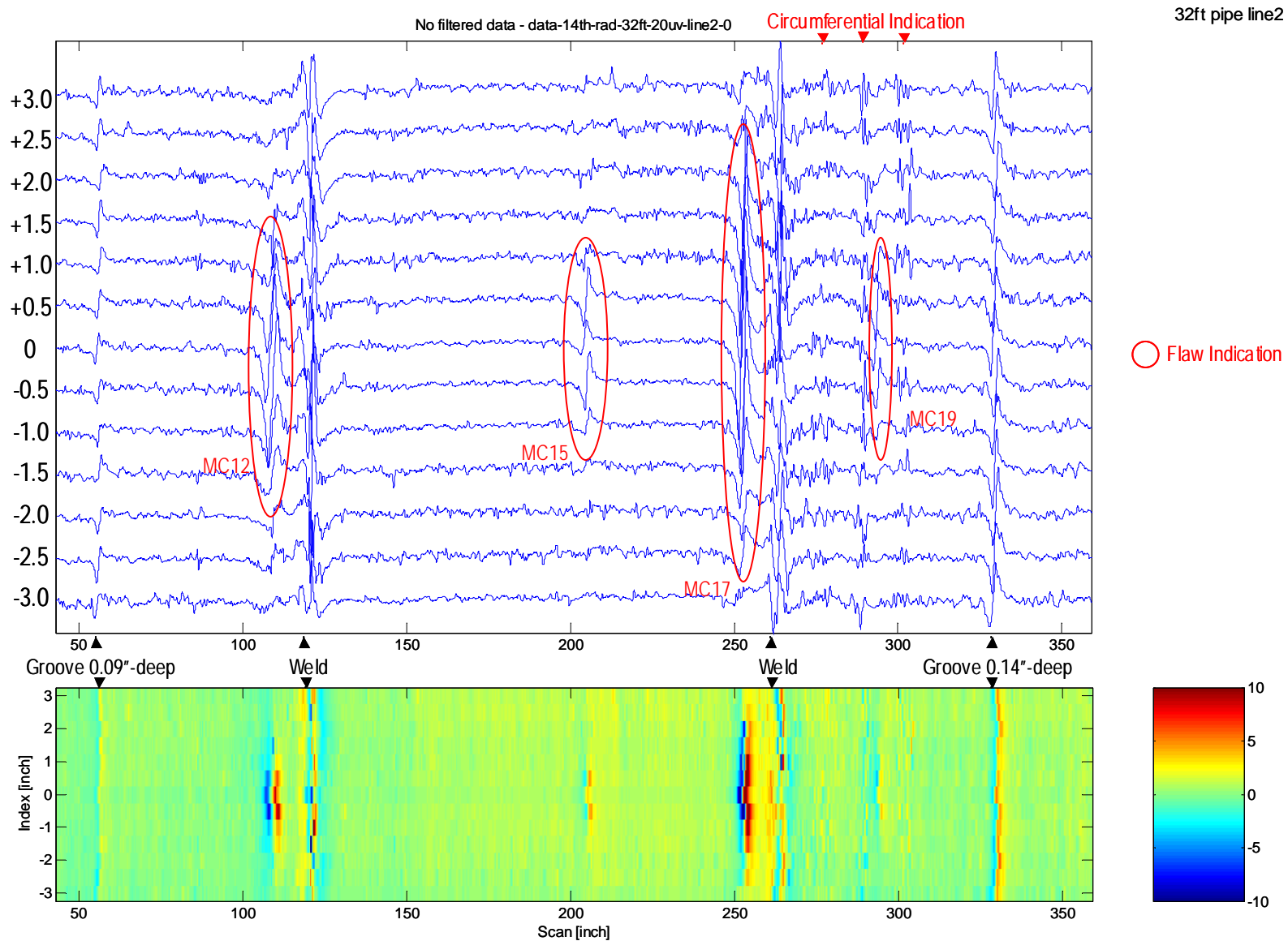
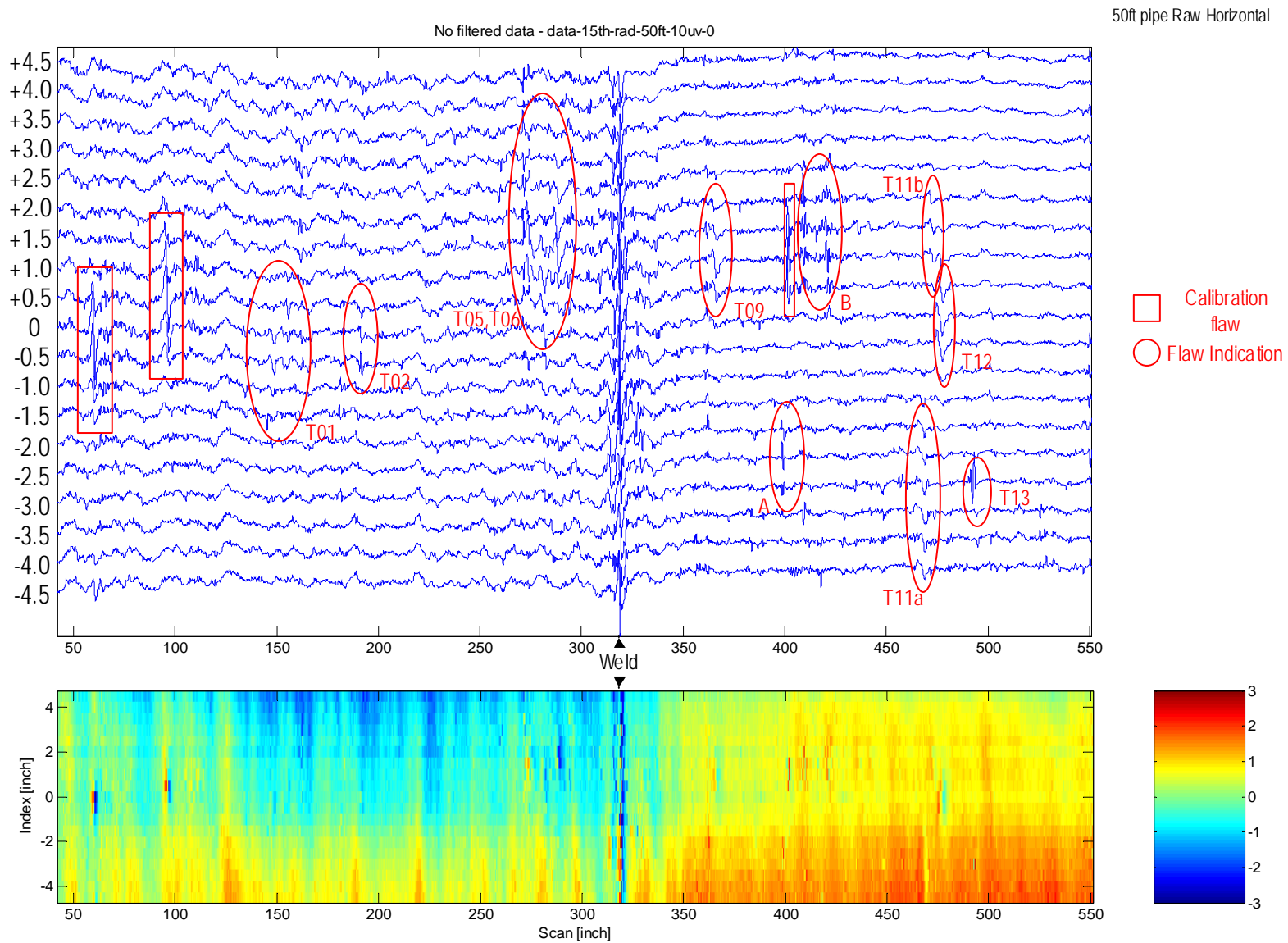**Figure 3. RFEC data from new seam-welded pipe with manufactured flaws — scan along Line 2**

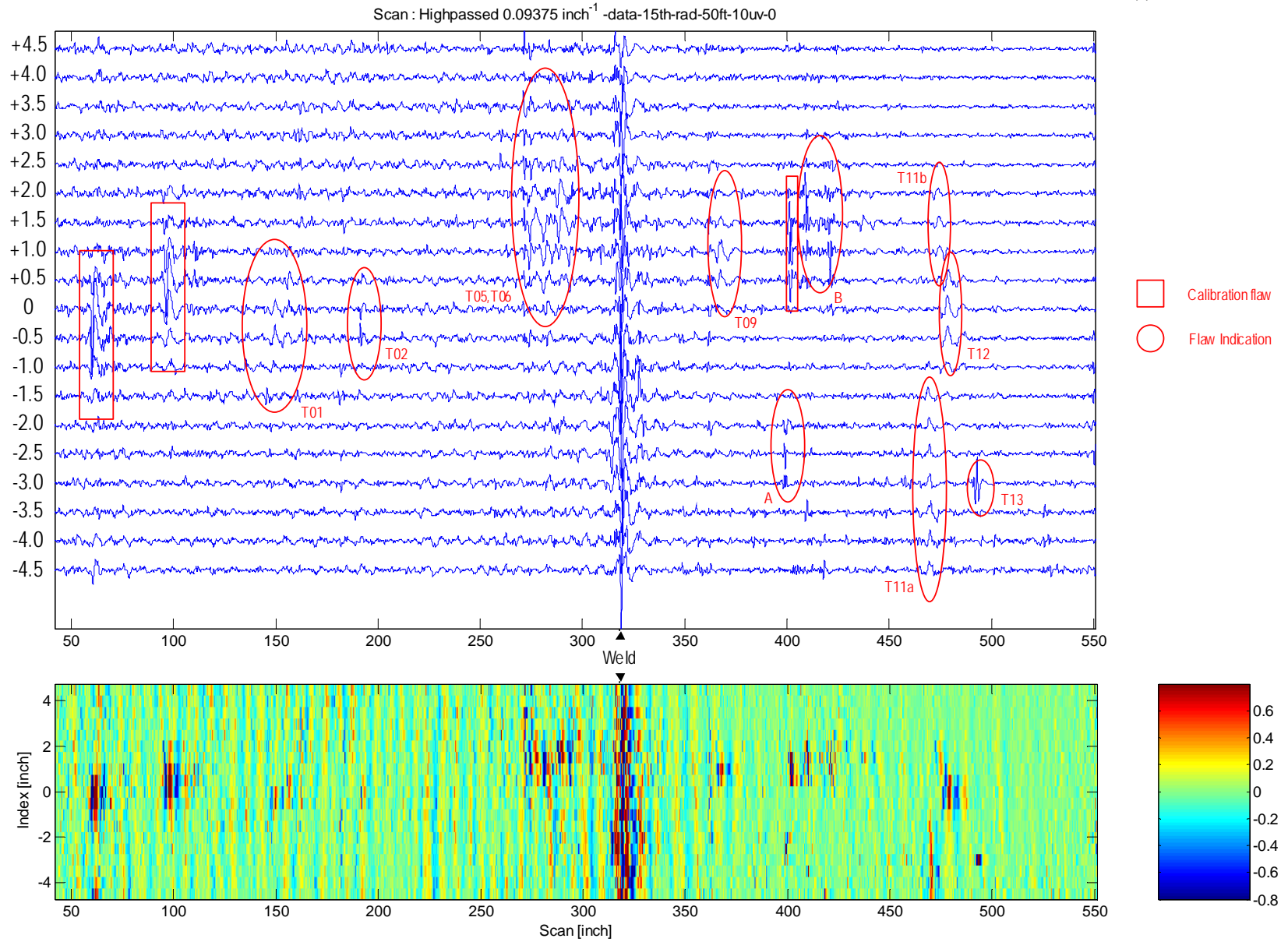**Figure 4. RFEC data from used seamless pipe with natural corrosion**

Figure 5. Filtered RFEC data from used seamless pipe with natural corrosion

Benchmarking of Inspection Technologies
Detection of Metal Loss - Page 1

Name:	Gary L. Burkhardt
Date:	9/14/2004
Company:	Southwest Research Institute
Sensor Design:	Collapsible RFEC

	CALIBRATION DATA						
	Calibration Metal Loss Location	Metal Loss Length & Width	Depth of Metal Loss	Radius of Curvature	Measured Length & Width of Defect	Measured Depth of Defect	Comments
	inches from end A	inches	inches	inches			
Natural Corrosion Pipe Sample (48' 2")							
Calibration T1:	60	1	0.3	0.557			
Calibration T2:	96	1.475	0.21	1.417			
Calibration T3:	401	1.475	0.21	1.417			
Manufactured Metal Loss Pipe Sample (32')							
Groove Defect 1:	55	0.5	0.09	0.25			
Groove Defect 2:	329	0.5	0.14	0.25			
Calibration MC01:	90	1.2 long x 3 wide	0.29	0.933			

	TEST DATA						
Pipe Sample:	**Manufactured Corrosion Sample**						
Defect Set:	12" Diameter, 0.358" Wall Thickness Pipe Sample with Manufactured Metal Loss						
	LINE 1						
Defect Number	Search Region (Distance from End A)	Start of Metal Loss Region from Side A	End of Metal Loss Region from Side A	Total Length of Metal Loss Region	Width of Metal Loss Region	Maximum Depth of Metal Loss Region	Comments
	inches	inches	inches	inches	inches	inches	
MC02	126" to 138"	130.83	133.26	2.43	2.5	0.06	
MC03	144" to 156"						
MC04	162" to 174"						
MC05	186" to 198"	191.31	192.93	1.62	2.5	0.16	
MC06	210" to 222"						
MC07	234" to 246"	239.10	240.99	1.89	1.5	0.12	
MC08	264" to 276"						
MC09	282" to 294"	286.08	287.70	1.62	3.0	0.22	
MC10	306" to 318"						

	Benchmarking of Inspection Technologies Detection of Metal Loss - Page 2					
Name:	Gary L. Burkhardt					
Date:	9/14/2004					
Company:	Southwest Research Institute					
Sensor Design:	Collapsible RFEC					
	TEST DATA					
Pipe Sample:	**Manufactured Corrosion Sample**					
Defect Set:	12" Diameter, 0.358" Wall Thickness Pipe Sample with Manufactured Metal Loss					
	LINE 2					
Defect Number	Search Region (Distance from End A)	Start of Metal Loss Region from Side A	End of Metal Loss Region from Side A	Total Length of Metal Loss Region	Width of Metal Loss Region	Maximum Depth of Metal Loss Region	Comments
	inches	inches	inches	inches	inches	inches	
MC11	78" to 90"						
MC12	102" to 114"	107.05	109.74	2.69	2.5	0.16	
MC13	138" to 150"						
MC14	174" to 186"						
MC15	198" to 210"	203.49	204.57	1.08	2.0	0.05	
MC16	222" to 234"						
MC17	246" to 258"	251.45	253.07	1.62	3.0	0.21	
MC18	272" to 284"						
MC19	288" to 300"	292.67	293.75	1.08	1.5	0.08	

<table>
<tr><td colspan="7" align="center">Benchmarking of Inspection Technologies
Detection of Metal Loss - Page 3</td></tr>
</table>

Name:	Gary L. Burkhardt
Date:	9/15/2004
Company:	Southwest Research Institute
Sensor Design:	Collapsible RFEC

TEST DATA	
Pipe Sample:	**Natural Corrosion Sample**
Defect Set:	12" Diameter, 0.31" to 0.38" Wall Thickness Pipe Sample with Natural Corrosion

Defect Number	Search Region (Distance from End A)	Start of Metal Loss Region from	End of Metal Loss Region from	Total Length of Metal Loss	Width of Metal Loss Region	Maximum Depth of Metal Loss Region	Comments
	inches	inches	inches	inches	inches	inches	
T01	144" to 156"	146.53	155.84	9.31	3.0	0.09	
T02	180" to 192"	191.11	191.87	0.76	1.0	0.11	
T03	216" to 228"						
T04	260" to 272"						
T05	272" to 284"	273.58	284.00	10.42	4.5	0.15	T05 defect extends into T06.
T06	284" to 296"	284.00	288.66	4.66	2.0	0.15	T05 defect extends into T06.
T07	296" to 308"						
T08	348" to 360"						
T09	360" to 372"	364.67	366.24	1.57	1.5	0.09	
T10	438" to 450"						
T11a	462" to 474"	465.56	469.03	3.47	2.0	0.05	Two separate defects in T11 area.
T11b	462" to 474"	471.54	473.39	1.85	2.0	0.04	T11b may be part of T12.
T12	474" to 486"	475.11	477.28	2.17	3.0	0.08	
T13	486" to 498"	492.32	493.22	0.90	0.5	0.29	Signal only on one scan line; difficult to characterize.
T14	500" to 512"						